Test-Derived Effective Emittance for Cassini Ml.] Blankets and Heat Loss Characteristics in the Vicinity of Seams[1]

by

Edward 1.1 in, James W. Stultz and Ronald T. Reeve
Jet Propulsion I .aboratory
California Institute of Technology
Pasadena, California

Abstract

The Cassini spacecraft is currently under development for a mission designed to explore Saturn and its rings, satellites and magnetosphere. Multilayer insulation (Ml .1) blankets on the spacecraft will experience temperatures in the wide range of -200 to 360°C. High temperat urc conditions will occur at the main engine under plume heating in conjunction with the 0.61 AU (Astronomical Unit) solar illumination, and near the RTG (Radioisotope Thermoelectric Generator) under the combined heating of the RTG (3900W) and 2.7 suns during a trajectory correction maneuver, 1 .ow temperature conditions arc more prevalent as the spacecraft will cruise, for the most part, in the shade of its sun-pointed high gain antenna. Besides reducing heat loss, the Ml.1 blankets will also serve, with standoffs, the purpose of micrometeoroid protection. Four major blanket layup configurations (referred to as MLI-A, -B, -C and -D, and described in Fig. 1) will be utilized on Cassini. Since definitive thermal properties for these layups were not available, thermal vacuum tests were conducted for their determination.

The tests involved suspending in a 1.Nz-cooled vacuum chamber a pair of heater-contro]]cd aluminum boxes that are each enclosed in an Ml.1 blanket, driving the test articles to steady state at several box/sink temperat urc sctt ings, and measuring input power to the boxes, as well as temperat ures on the boxes and M LI blankets at various locations. Figure 2 shows photographs of MLI-A, -B, and -C, and Fig. 3 displays the outer and inner blankets of MLI-D. Ml .1-A, -B, and -C are of dimensions 1 2. S" cubed, and Ml ,1-C 9.5" cubed. Figure 4 illustrates the blanket and the aluminum box with Mylar standoffs, noting that the latter was typically enclosed by the former and heated from within during a test.

Among other things, the tests have yielded effective emittance for the four blanket layups at several temperature settings; shown that the embossed Kapton MI.1 is "leakier" than the Kapton-Mylar hybrid Ml,1; validated the superior performance of a duo-blanket which avoids through scams; quantified heat]oss in the vicinity of scams, elucidating a major Ml.1 heat loss mechanism; revealed greater radiative/conductive heat transfer between the hardware and the

[1]The work described in this paper was carried out by the Jet]'repulsion 1,abm'story under a contract with the National Aeronautics and Space Administration. The paper is submitted to the AIAA 29th Thermophysics Conference, to be held in San Diego, CA, on June 1 9-22, 1995.

inner layer of an Ml.1 than commonly presumed; and established that these four MLI layup designs will be able to provide adequate thermal performance for the Cassini spacecraft throughout its mission.

Effective Emittance. The effective emittance data derived from the tests arc presented in Table 1. The heat dissipation (()), box temperature ('1'$_1$,) and chamber shroud temperature (T_s) for each test phase are tabulated, These test data were used to compute the traditional ϵ_{eff} (effective emittance, as defined in '1'able 1). The "averaged" temperatures for the blanket outer and inner layers (T. and T_i) arc also listed; T_o is consistent with heat balance calculations, and 'J'$_i$ is a weighted average involving some judgment and may entail a small error. The effective emittance based on the box and outer-la yer temperatures ($\epsilon^*_{eff\text{-}bo}$), and the effective emittance based on the inner- and outer-layer temperatures ($\epsilon^*_{eff\text{-}io}$) were then computed, using the definitions noted in Table 1. Values of the radiation conductor between the Ml.] outer-]aycr and the chamber shroud (GO,), and those bet ween the box and the M LI inner-]a ycr (G_{bi}) are also prcscntcd.

Discussions on effective emittance in the MLI literature usually do not make a clear distinction between the traditional definition and that based on the Ml.] inner- and outer-layer temperatures. The results of "1'able 1 show that a clear distinction is necessary, however. Physically, the effective emittance based on the inner- and outer-layer temperatures is an intrinsic characteristic of the blanket layup, while the traditional effective emittance incorporates also effects of the hardware surface emissivity, the Ml.] inner- and outer-layer emissivity, the hardware-to-b]aJlket gap geometry, and the emissivity and geometry of the sink (e.g., the chamber shroud). The base area (whether of the box or Ml .1) has to be considered when making comparison of the various effective emittance values, as must other physical parameters (e. g., temperature effect).

As far as needs of therms] modeling for Cassini arc concerned, two distinct situations call for effective emittance defined in both ways. Namely, (1) hardware covered by Ml.] directly, or hardware covered by Ml.1 which is spaced off by the Mylar standoffs (for micrometeoroid protection); and (2) MLI used in a tent-like or drape-like configuration (e. g., the fields and particles pallet and the propulsion module subsystem), where it is spaced off the spacecraft hardware by an appreciable distance. In the first situation, the common modeling approach assigns onc node to the hardware surface, and one node to the MLI outer-layer, and applies the traditional ϵ_{eff} to calculate the conductor between the two nodes. Strictly speaking, it is $\epsilon^*_{eff\text{-}bo}$ that should be used in this connection. However, numerical values for the two arc so close, as 'J'able 1 indicates, that using the traditional ϵ_{eff} is quite acceptable. In the second situation, the common modeling approach assigns a node to the inner-]aycr, and a node to the outer-layer of the MLI, in addition to whatever modeling is suitable for the hardware; the radiative interchange bet wccn the hardware and the inner-layer of the MLI is calculated by a TRASYS or N] :VADA model, and the conductor bet ween the inner- and outer-layer needs to be computed by u sing $\epsilon^*_{eff\text{-}io}$ (note that the traditional ϵ_{eff} would not be appropriate here!)

The values of the traditional ϵ_{eff} as presented in Table 1 show a high degree of repeatabil it)', considering that four different blanket layups were involved in three d ifferent test phases, that

chamber breaks and rearrangement of test articles occurred between test phases, and that the tests were conducted at several temperat urc settings. The embossed Kapton layup (i .e., Ml .J-B) was shown to be 19% "leakier" than the Kapton-Mylar hybrid layup (MLJ-A), and the duo-blanket layup (MI .1-D) exhibited superior performance characteristics made possible by, among other things, avoidance of through scams.

1 Ieat Loss Characteristics in the Vicinity of Seams. Early test phases showed that MLJ temperatures near box corners are dramatically different from those in the middle of surfaces. By placing additional thermocouples on the test articles, subsequent test phases produced temperature distributions such as exemplified by Fig. 5. It was noted that on the blanket inner layer, the temperature at the scam can be more than 30°C lower than in the middle, while on the outer layer, the scam temperature can be higher than the center temperature by more than 70°C. It is reasoned that the stitches have pinched together the Ml.1 layers at the scam and caused a "thermal short"; this brings the outer- and inner-layer temperatures closer to each other at the scam than clsewhcrc. Utilizing the outer layer temperatures and emissivity, and the shroud temperature, the local heat losses can be computed, and the results are presented in Fig. 6 as a function of distance from the scam. The heat loss varies from less than 3 W/m^2 in the middle to almost 30 W/m^2 at the scam. With the understanding that lateral (i .c., in-layer) heat transfer is negligible, local effective emittance was then calculated using the inner and outer layer temperatures and the heat losses of Fig. 5. The results arc plotted in Fig. 6, where it is seen that local effective emittance varies from a low of less than 0.01 to a high of almost 0.15.

The average effective emittance must lie somewhere in bet ween, depending on the size of the blanket, and other hard ware configuration parameters. The larger the blanket, the more the low emittance in the middle will weigh on the average. It is thus clear that, in selecting a value for the MLJ effect ive emittance, analysts must consider the size and other geometric factors of the Ml.1, and how the MLJ will be fabricated and assembled. Figure 7 gives suggestions as to the upper and lower bounds of effective emit [ante that one may select in conducting sensit ivity studies, as well as points to a way of improving MLJ thermal performance; i.e., by eliminating or minimizing the scam 1o SSCS. Ml .J-D has provided such an example.

With highlights given above, the paper will provide details on the test articles, test setup, test procedures, test results, and data analysis and interpretation. The clarification of the various definitions of MI.1 effective emittance and their appropriate applications, as well as the quantification of heat 1oSSCS in the vicinity of scams arc believed to be new results not yet reported before in the MI.] literature.

Cassini MLI Tests

Computation of Effective Emittance

Thermal Blanket	Test Phase	Q (W)	Tb (C)	Ts (C)	Eeff, Traditional	Gos (W/K^4)	To (C)	Ti (C)	Eeff*-be, per A(box)	Eeff*-10. per A(MLI)	Gbi (W/K^4)
MLI- A	1a	3.449	20.4	-186.9	0.026	2.16E-08	. - 1 5 2 : .	3.1	0.027	0.018	2.15E-09
	1b	5.205	54.6	-186.5	0.025	2.16E-08	-141.9	37.5	0.026	0.017	2.34E-09
	1c	4.733	-"54.7	-102.2	0.025	2.16E-08	-92.2	39.6	(?.0'25	0.016	2.38E-09
	1d	,2.998	22.3	-104.6	0.025	2.16E-08	-97.8"	7.8"	0.025	0.017	2.16E-09
	2a	3.006	23.7	-98.0,	0.025	2.16E-08	-91.9	9.7	0.025	0.017	2.20E-09
	2b	3.551	21.8	-184.3	0.027	2.16E-08	-150.5	4.6	0.027"	0.018	2.20E-09
	2c	5 260	50.7	-184.0	0.027	2.16E-08	-140.9	33.0	0.028	0.018	2.38E-09
	3a	3.428	21.9	-184.4	0.026	2. 16E-08	-151.3	5.1	0.026	0.018	2.16E-09
	3b	3.043	22.0"	-96.8'	0.026	2. 16E-08	-90.7	8.1	0.026	0.017	2.29E-09
	3c	4.595	50.0	-99.2	0.026	2. 16 E-08""""	-89.9	35.2	0.026	0.017	2.46E-09
	3d	4.595	50.2	-186.0	0.024	2.16E-08	-144.9	33.0	().024-	0.016"	2.14E-09
MLI B	2a	3.006	14.3	-101.4	0.028	2.64E-08	-96.0	-8.0	0.029	0.022	!.60E-09
	2b	4.087	21.4	-184.6	0,031,	2.64E-08	-151.8	-6.7	0.031	0.025-	1.64E-09
	2c	6.011	50.2	-184.4	0.031	2.64E-08 "	-142.6	23.0	0.032	0.024	!.86E-09
MLI-C	1a	3.450	21.8	-186.6	0.026	1.26E-08	-138.4	-5.6	0.027	0.037	!.41E-09
	1b	5.035	56.6	-186.4	0.024	1.26E-08	-127.0	30.8	0.025	0.032	1.53E-09
	1c	4.686	~6.4	-[02.2'	0.024	1 .26E-08	-86.0	34. !	0.025	0.031:	1.63E-09
	1d	3.003	24.3	-104.2	0.024	1.26 E-08'	-93.0	o. !--	0.025	0.034	!.33E-09
MLI-D	3a	1 .200	21.9	-187.5	0.009	2 . 16E-08	-170.9	14.5	0.009	0.005	1.64E-09
	3b	1.228	21.9	-98.4	(?.0"10.	2.16E-08	-95.8	14.4	0.010	0.006	1.66E-09
	3c	2.101	49.4	-103.6	0.012	2.16E-08	-98.8	40.8	0.012	0.007	1.89E-09
	3d	1.951	53.1	-186.4	0.010	2.16E-08	-163-1	43.3	n.010	0.006	1.50E-09
How numbers are obtained			Test data			Computation		Processed test data		Computation	

NOTE:

$$\epsilon_{eff} \equiv \frac{Q}{A\,\sigma\,(T_1^4 - T_2^4)} \qquad \text{(Effective emittance)}$$

For E_{eff} (traditional), $A = A_{box}$, $T_1 = T_{box}$, $T_2 = T_{shroud}$

For E_{eff}*-bo, $A = A_{box}$, $T_1 = T_{box}$, $T_2 = T_{outer\text{-}layer}$

For E_{eff}*-io, $A = A_{MLI}$, $T_1 = T_{inner\text{-}layer}$, $T_2 = T_{outer\text{-}layer}$

Box and MLI areas:

$A_{box} = 486\ in^2$

$A_{MLI\text{-}A} = A_{MLI\text{-}B} = A_{MLI\text{-}D} = 925\ in^2$

$A_{MLI\text{-}C} = 532\ in^2$

CAUTION: Exercise sound **judgment** when **applying** these test-derived **values** to conditions different from those of the tests!

Table 1. Effective Emittance Derived from Test Data for Four Blanket Layups

EL 2/11/94

Definitions:

MLI-A: IKNA + 5EA(2)K + 15A(2)M/N -1 A(2)K, with micrometeoroid spacers (standard blanket layup)
MLI-B: CKA + 20 EA(2)K + A(2)K, with micrometeoroid spacers (blanket layup for high-temperature locales)
MLI-C: IKNA + 5EA(2)K + 15 A(2)M/N + A(2)K, without micrometeoroid spacers
MLI-D: IKNA -t 5EA(2)K + 15 A(2) M/N -t A(2)K, with inner and outer blankets and staggered seams, and with micrometeoroid spacers

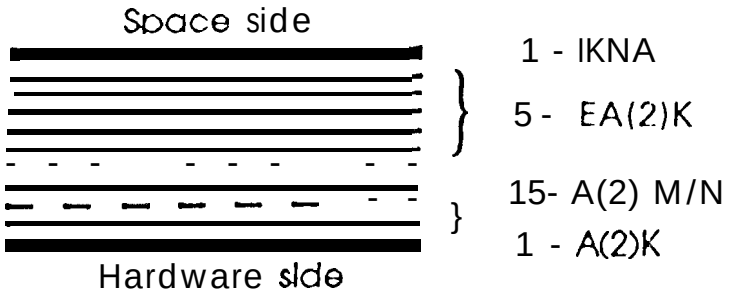

MLI-A

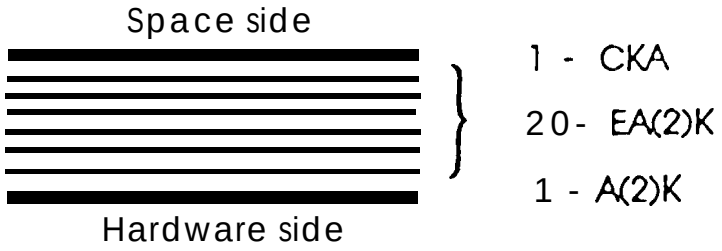

MLI-B

NOTES:

IKNA = 1/2 mil - ITO Kapton-Nomex Scrim, aluminized
EA(2)K = 1/3 mil - embossed aluminized (both sides) Kapton
A(2)K = 1 mil - aluminized (both sides) Kapton
CKA = 1 mil - Carbon filled Kapton-aluminized
A(2)M/N =- 1/4 mil - aluminized (both sides) Mylar with Dacron net

Figure 1. Description of MLI Layups Tested

Figure 2. Photographs of MLI-A, MLI-B and MLI-C (from Left to Right)

Figure 3. Photograph of MLI-D (The Outer Blanket Is Box-Shaped; The Inner Blanket Unfolded)

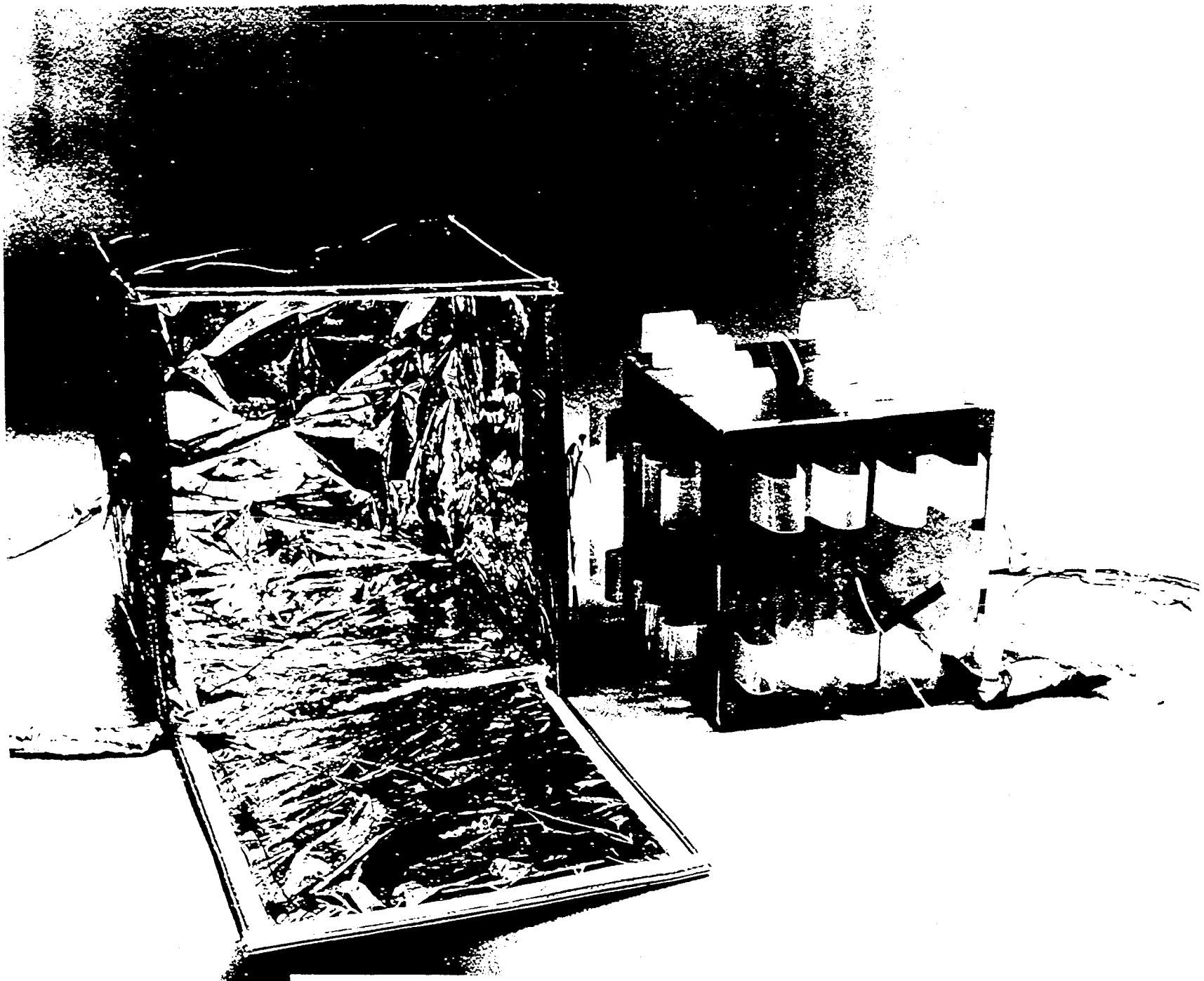

Figure 4. MLI Blanket and Aluminum Box with Mylar Standoffs

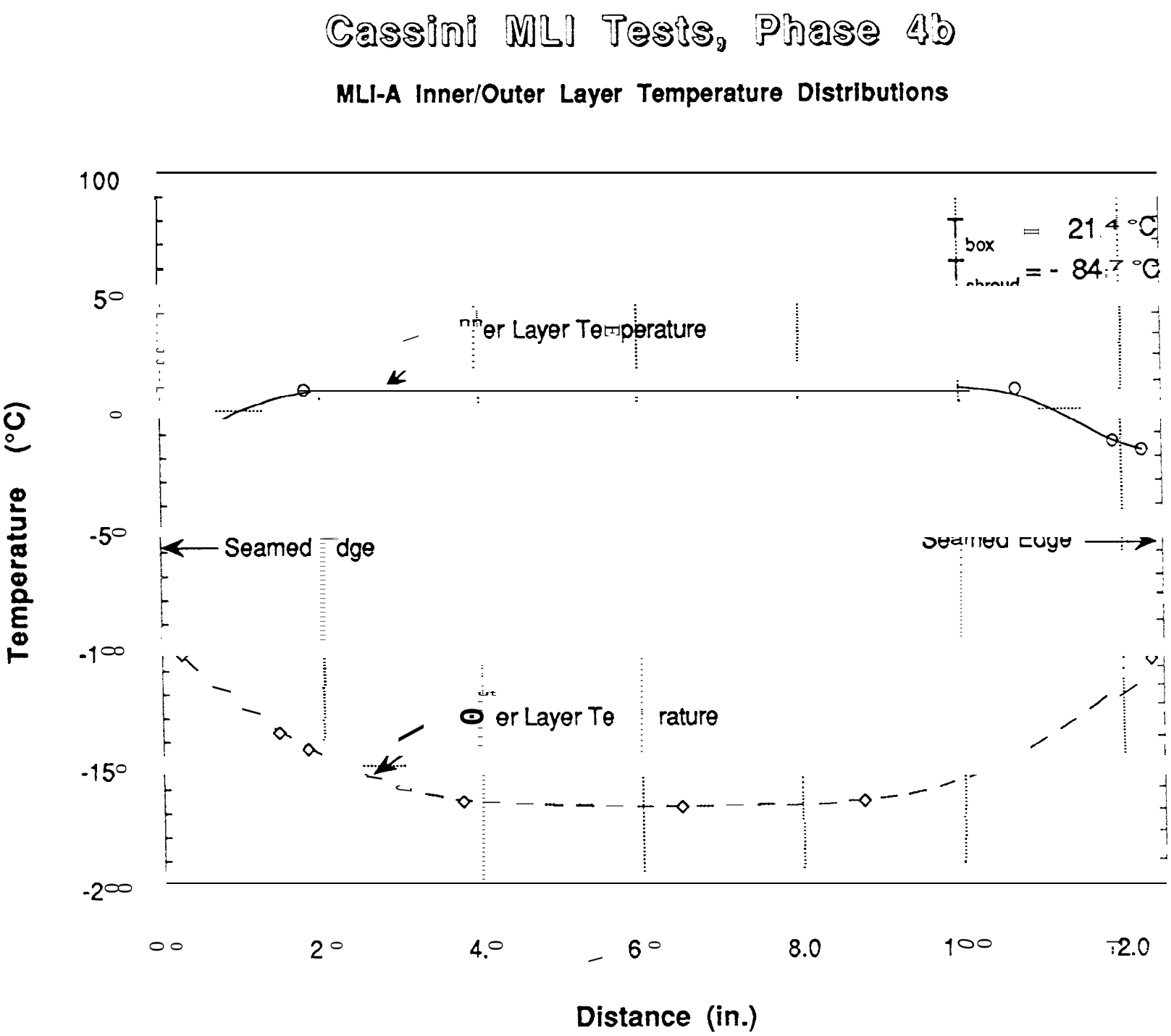

Figure 5. MLI Temperature Distribution as Function of Distance from Seam

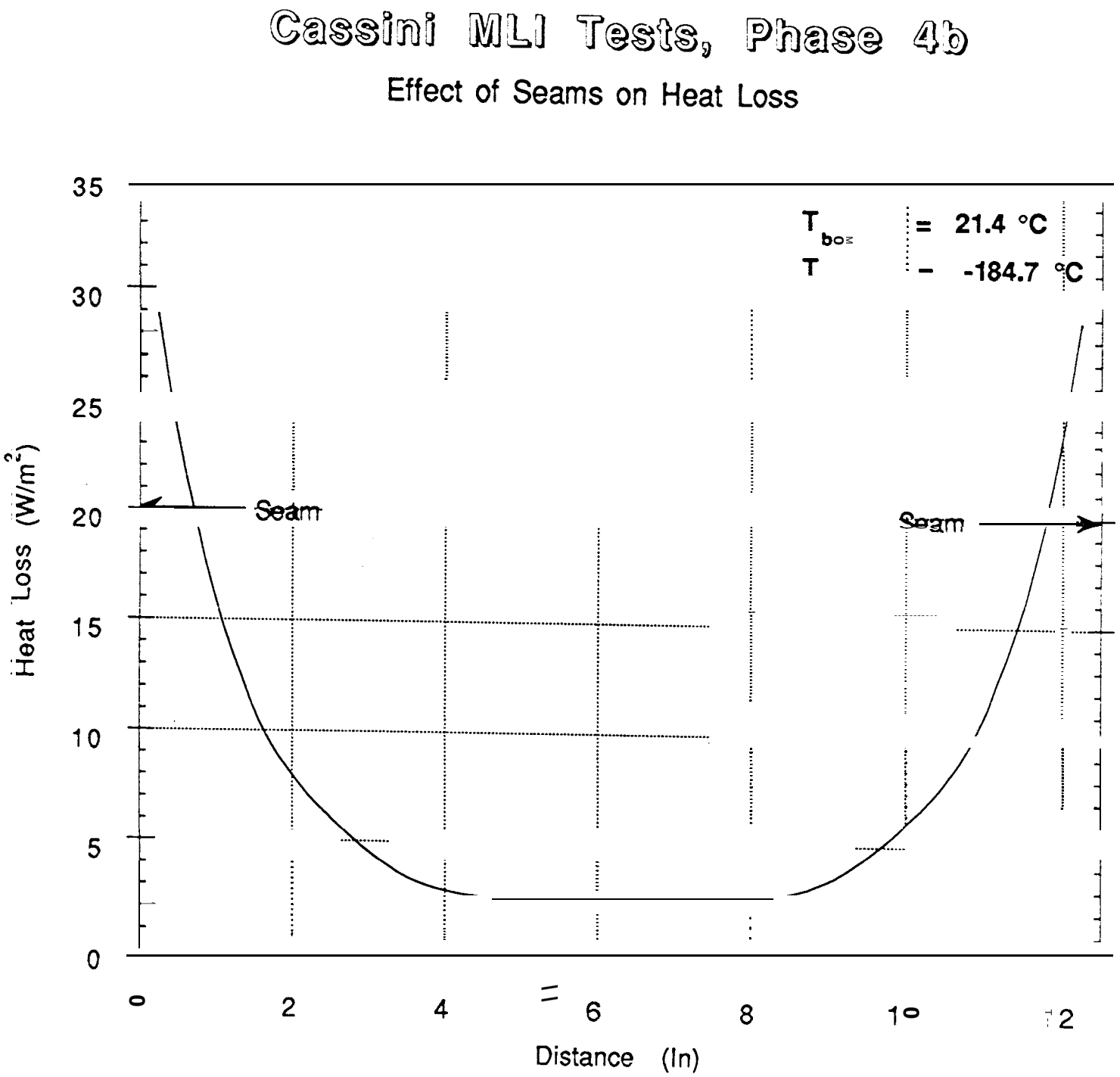

Figure 6. MLI Heat Loss as Function of Distance from Seam

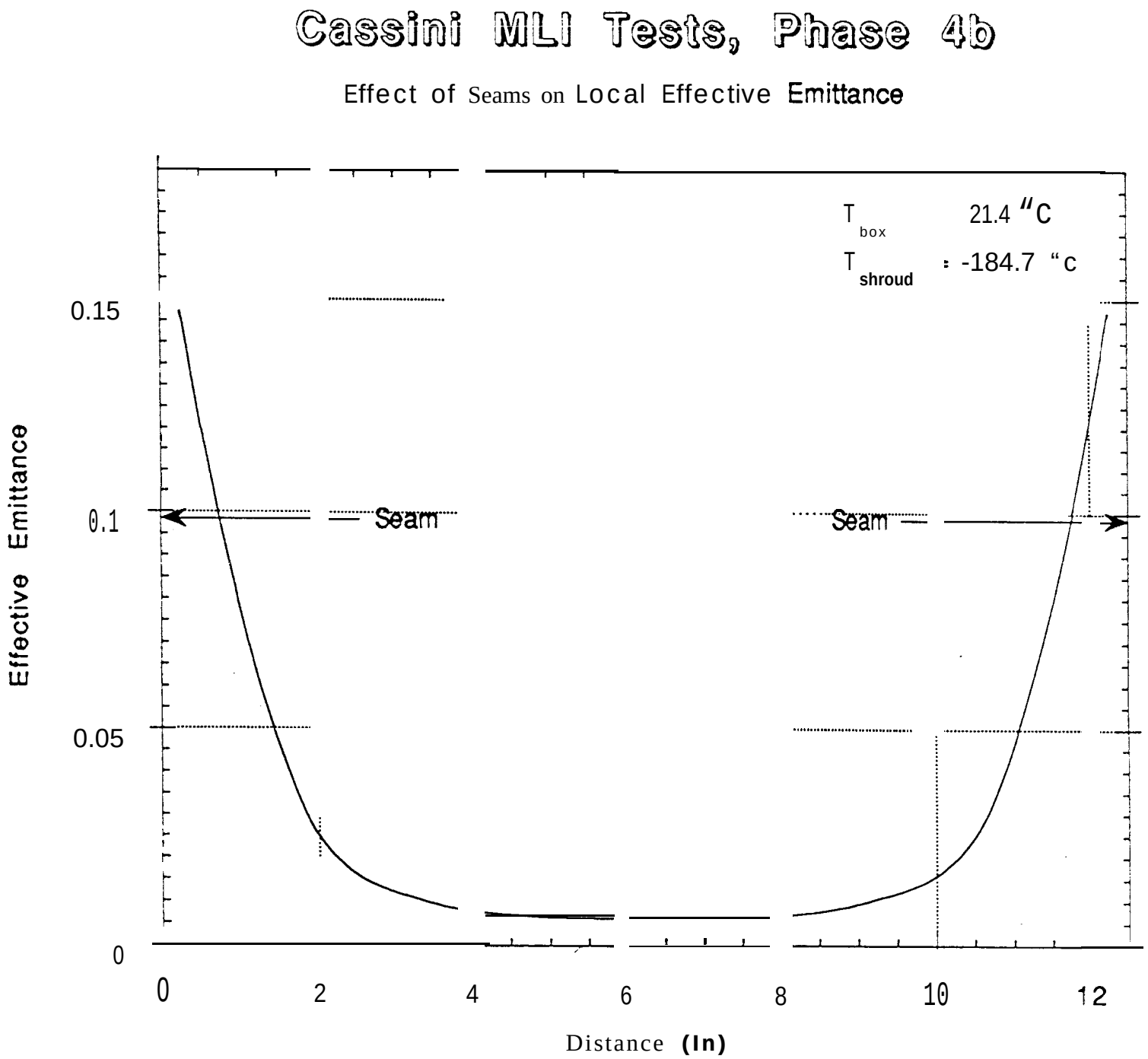

Figure 7. MLI Local Effective Emittance as Function of Distance from Seam